

Mouse *Hyal3* encodes a 45- to 56-kDa glycoprotein whose overexpression increases hyaluronidase 1 activity in cultured cells

Richard Hemming^{2,3}, Dianna C. Martin^{2,3}, Elzbieta Slominski³, James I. Nagy⁴, Andrew J. Halayko^{4,6}, Steven Pind³, and Barbara Triggs-Raine^{1,3,5,6}

³Department of Biochemistry and Medical Genetics; ⁴Department of Physiology; ⁵Department of Pediatrics and Child Health, The University of Manitoba, 770 Bannatyne Ave., Winnipeg, MB R3E 0W3; and ⁶Manitoba Institute for Child Health, 715 McDermot Ave., Winnipeg, MB R3E 3P4, Canada

Received on April 3, 2007; revised on January 25, 2008; accepted on January 26, 2008

Hyaluronidases are enzymes that mediate the breakdown of hyaluronan (HA), a large polysaccharide abundant in the extracellular matrix of vertebrate tissues. Six genes have been predicted to encode hyaluronidases in humans, but the protein products of only *SPAM1*, *HYAL1*, and *HYAL2* have been characterized. We have now expressed the mouse *Hyal3* gene product, hyaluronidase 3 (Hyal3), in Baby Hamster Kidney (BHK) cells and demonstrated the presence of multiple forms of Hyal3 ranging from ~45 to 56 kDa in expression lysates. Complete and partial digestions of the expressed protein with PNGase F showed three *N*-linked oligosaccharides accounted for all forms of Hyal3 detected in expression lysates. Most of these oligosaccharides were Endo H sensitive, indicating that they were high mannose or hybrid *N*-linked oligosaccharides. Subcellular fractionation of Hyal3-expressing BHK cells by density gradient centrifugation revealed most Hyal3 in a low-density vesicular population. Low levels of Hyal3 were detected in higher density vesicles, but no colocalization with the late endosomal/lysosomal marker Lamp1 was found by immunofluorescence microscopy. BHK cells stably expressing Hyal3 had increased acid-active hyaluronidase activity, but no such activity was detected when Hyal3 was transfected into Hyaluronidase 1 (Hyal1)-deficient fibroblasts. Overexpression of Hyal3 in BHK cells increased the Hyal1 protein and mRNA levels, suggesting that the increased hyaluronidase activity in these cells was due to Hyal1 rather than Hyal3. The results indicate that Hyal3 overexpressed in cultured cells lacks intrinsic hyaluronidase activity and that Hyal3 may contribute to HA metabolism by augmenting the activity of Hyal1.

Keywords: endoglycosidase/Hyal1/Hyal3/hyaluronan/hyaluronidase

¹To whom correspondence should be addressed: Tel: +1-204-789-3218; Fax: +1-204-789-3900; e-mail: traine@ms.umanitoba.ca

²These authors contributed equally to this work.

Introduction

Hyaluronidases (EC 3.2.1.35) are members of the glycoside hydrolase family 56, a group of enzymes that cleave hyaluronan (HA) at the β 1-4 linkage between *N*-acetyl- β -D-glucosamine and D-glucuronic acid to generate smaller oligosaccharides (Stern 2003). These oligosaccharides are further degraded, presumably through the action of the lysosomal exoglycosidases β -hexosaminidase and β -glucuronidase (Roden et al. 1989). In vertebrates, HA is a ubiquitous macromolecule and is most abundant in connective tissues such as synovial fluid and skin (Fraser et al. 1997). Although the half-life of HA varies depending upon its location and interactions with extracellular matrix proteins and proteoglycans, it has been estimated that about one-third of HA in the body is catabolized and replaced each day (McCourt 1999). Understanding mechanisms responsible for HA synthesis and degradation is essential given the critical structural and functional roles of HA in embryonic development (Toole 2000), cancer progression (Kosaki et al. 1999), and many other physiological processes relevant to health and disease (Lee and Spicer 2000).

The existence of multiple hyaluronidase enzymes in mammalian tissues was evident several decades ago (Bowness and Tan 1968). However, the characterization of these enzymes was impeded by their generally low endogenous levels and by difficulties in assaying their activity. Based on human genome analysis, six genes are predicted to encode hyaluronidases and one related pseudogene has been identified. These genes form two clusters: *HYAL1*, *HYAL2*, and *HYAL3* on human chromosome 3p21.3 (mouse chromosome 9F-F2) and *HYAL4*, *SPAM1*, and *HYALP1* on human chromosome 7q31.3 (mouse chromosome 6 A2) (Csoka et al. 2001). In mouse, one additional gene, *Hyal5*, has also been identified downstream of the cluster on chromosome 6 (Baba et al. 2002). The human/mouse *HYAL1/Hyal1*, *HYAL2/Hyal2*, and *HYAL3/Hyal3* genes are each broadly expressed (Csoka et al. 1999; Shuttleworth et al. 2002), and their protein products, hyaluronidase 1 (HYAL1/Hyal1), hyaluronidase 2 (HYAL2/Hyal2), and hyaluronidase 3 (HYAL3/Hyal3), respectively, are thought to contribute as house-keeping enzymes in HA catabolism.

HYAL2 was originally characterized as an acid-active lysosomal enzyme that degrades high molecular mass HA to 20-kDa fragments (Lepperdinger et al. 1998). However, subsequent studies showed that *HYAL2* has a glycosylphosphatidylinositol (GPI)-anchored form that localizes to the outer membrane of cells (Rai et al. 2001). This form was shown to interact with a Na^+ - H^+ exchanger that creates an acidic microenvironment both inside and outside the cell (Bourguignon et al. 2004). It was suggested that *HYAL2* initiates the breakdown of HA outside the cell and that partially degraded products are internalized to

cellular compartments, where degradation is continued by other enzymes, including an acid-active HYAL1 (Frost et al. 1997). The participation of HYAL3/Hyal3 in HA catabolism has been proposed based on its broad, albeit weak expression in multiple tissues (Csoka et al. 1999; Shuttleworth et al. 2002), and on an observation that an in vitro translated form has acid-active (pH 4.2) hyaluronidase activity using an ELISA-like assay (Lokeshwar et al. 2002).

The genes in the second group, *HYAL4/Hyal4*, *SPAM1/Spam1*, and *HYALP1/HyalP1* in humans/mice and *Hyal5* in mice, exhibit either tissue-specific expression or no functional protein. *SPAM1* expression is largely limited to sperm, where it is thought to have an important role in fertilization (Gmachl et al. 1993). The *SPAM1*-encoded PH-20 is well characterized and exists both as a neutrally active GPI-anchored protein on the sperm outer membrane (Meyer et al. 1997) and as an acid-active proteolytically processed form in the sperm acrosome (Meyer et al. 1997; Seaton et al. 2000). *Hyal5* is thought to have functions similar to PH-20 (Kim et al. 2005; Reitingner et al. 2007). Little is known about the remaining hyaluronidases; *Hyal4* is expressed in the placenta and was suggested to be a chondroitinase (Csoka et al. 2001), and the capacity of *HyalP1* to degrade HA is currently controversial (Miller et al. 2007; Reitingner et al. 2007).

Evidence indicating a role for multiple members of the hyaluronidase family in HA catabolism derives from studies of a patient with the lysosomal storage disorder mucopolysaccharidosis IX (MPS IX) (Natowicz et al. 1996). We found that this disorder resulted from a complete deficiency of HYAL1 activity due to mutations in the *HYAL1* gene (Triggs-Raine et al. 1999). Considering the broad distribution and diverse functions of HA, this patient had a relatively mild phenotype, suggesting that other hyaluronidases may compensate for HYAL1 deficiency. HYAL3 is a candidate for such compensation, based on its expression in a broad range of tissues. As a first step in assessing the potential role of murine Hyal3 in HA metabolism, we expressed this protein in Baby Hamster Kidney (BHK) cells and Hyal1-deficient fibroblasts, and characterized its molecular forms, subcellular localization, and activity.

Multiple forms of Hyal3 resulting from differences in N-linked glycosylation were identified. The majority of Hyal3 was found in low-density vesicles using density gradient centrifugation, with only small amounts in regions of the gradient corresponding to the late endosomes/lysosomes. This was consistent with immunofluorescence microscopy where Hyal3 was detected in punctate cytoplasmic vesicles and in intensely labeled perinuclear structures, neither of which colocalized with Lamp1. Surprisingly, increased acid-active hyaluronidase activity detected in BHK cells overexpressing Hyal3 did not correlate with levels of Hyal3 protein expression. Instead, BHK cells stably expressing Hyal3 were shown to have increased levels of Hyal1 protein and mRNA, which could account for the increased hyaluronidase activity in these cells, while Hyal3 expressed in Hyal1-deficient fibroblasts possessed no detectable hyaluronidase activity under our experimental conditions.

Results

Characterization of anti-Hyal3 antibody

To investigate the murine Hyal3 protein, we used an affinity-purified antibody generated against a 14-amino-acid internal

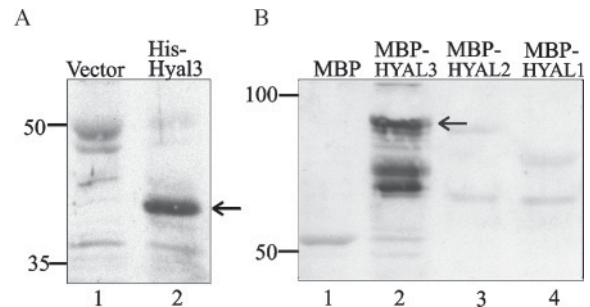


Fig. 1. Characterization of the anti-Hyal3 antibody. Extracts were prepared from *E. coli* expressing hyaluronidase fusion proteins or vector controls. The MBP-HYAL2 and MBP-HYAL1 fusion proteins were affinity-purified. Aliquots of the extracts or purified fusion proteins were separated by SDS-PAGE and analyzed by immunoblot with anti-Hyal3. Panel A: immunoblot showing detection of the mouse Hyal3 fusion protein (arrow, lane 2) that was not detected in lysates from *E. coli* expressing the empty pQe80L vector (lane 1). Panel B: immunoblot showing detection of the human HYAL3 fusion protein (arrow, lane 2) that was not detected in cells expressing MBP alone (lane 1). Anti-Hyal3 did not recognize either MBP-HYAL2 (lane 3) or MBP-HYAL1 (lane 4). Molecular mass markers in kDa are indicated on the left of the panels.

peptide corresponding to a sequence in murine Hyal3 (Invitrogen/Zymed, Camarillo, CA). The selected peptide spans a region of mouse Hyal3 that is least conserved among the mouse hyaluronidase proteins, with only 1 of 14 amino acids shared among these proteins. Immunoblot analysis was used for assessing reactivity of the antibody toward amino acids 1–412 of mouse Hyal3 and amino acids 1–417 of human HYAL3, and lack of reactivity toward amino acids 1–289 of human HYAL1 and amino acids 113–420 of human HYAL2. All of the proteins were produced as His- or maltose-binding protein (MBP)-fusions in *Escherichia coli* (*E. coli*) and contained the region that corresponds to the Hyal3 peptide selected for antibody production, although the region is poorly conserved in the HYAL1 and HYAL2 fusion proteins. The antibody recognized both the mouse Hyal3 (Figure 1, panel A, lane 2) and human HYAL3 (Figure 1, panel B, lane 2) fusion proteins, but did not cross-react with either the human HYAL2 or HYAL1 fusion proteins (Figure 1, panel B, lanes 3 and 4), nor was there detection of Hyal3 in bacterial extracts expressing vector only (Figure 1, panels A and B, lane 1). Antibody reaction was far weaker with human compared with mouse Hyal3 such that a several-fold dilution of mouse Hyal3 expression lysate was required to produce the same signal as that observed in the detection of the human HYAL3 fusion protein. This differential detection was not due to differences in expression efficiency of mouse versus human HYAL3 because protein counterstaining showed an absence of a Coomassie blue band representing mouse Hyal3, whereas human HYAL3 was readily visible by Coomassie blue (not shown). The poor reaction of the antibody with the human HYAL3 fusion protein is consistent with differences in amino acid sequence (10 of 14 amino acids identical) between the human and mouse Hyal3 proteins in the region corresponding to the peptide antigen.

Characterization of the mouse Hyal3 protein

To characterize the product of the mouse *Hyal3* gene, a vector encoding full-length mouse Hyal3 cDNA (pIRESHyal3) was

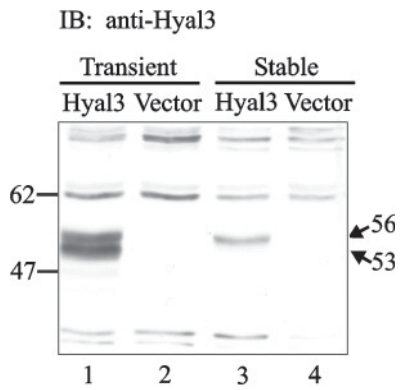


Fig. 2. Analysis of Hyal3 forms expressed in BHK cells. Immunoblot (IB) showing detection of Hyal3 with the anti-Hyal3 antibody in lysates from BHK cells transiently (lane 1) or stably (lane 3) transfected with the Hyal3 expressing the vector pIRESHyal3 and the absence of detection in the empty vector (pIRESneo)-transfected cells (lanes 2 and 4). Transiently transfected cells contain 53- and 56-kDa forms of Hyal3, and stably expressing cells show predominantly the 53-kDa form. All lanes were loaded with 50 μ g of protein. The position of molecular mass markers is shown in kDa on the left of the panel.

transiently transfected into BHK cells. Immunoblot analysis of the BHK-expressed protein with anti-Hyal3 revealed two major bands migrating at about 53 and 56 kDa (Figure 2, lane 1), which were not present in cells transfected with the pIRESneo vector alone (Figure 2, lane 2). Two stable lines expressing Hyal3 were isolated (BHK/Hyal3 cells), and the cell line with the highest level of mouse Hyal3 expression was used for further analysis of the various forms and activity of the mouse Hyal3 protein. The stable cells were found to express primarily the 56-kDa form (Figure 2, lane 3) and no Hyal3 was detected in cells stably transfected with the pIRESneo vector alone (Figure 2, lane 4). However, up to four bands were sometimes detected in BHK/Hyal3 lysates, such as in the lysate used for the subcellular fractionation (see *Localization of Hyal3 by density gradient centrifugation and immunofluorescence microscopy*).

The presence of several forms of Hyal3 in transient transfection lysates and in some stable expression lysates suggested that multiple forms of Hyal3 may be biologically relevant. To determine the biochemical basis for these various forms, we tested the effect of deglycosylation with peptide *N*-glycosidase (PNGase) F and endoglycosidase (Endo) H on the stably expressed Hyal3 protein. Treatment of the 56-kDa form of Hyal3 (Figure 3, panels A and B, lane 2) with either PNGase F or Endo H produced one major band of approximately 45 kDa (Figure 3, panels A and B, lane 1). This molecular weight is slightly larger than that predicted for unmodified Hyal3 (43.4 kDa) after cleavage between amino acids 22 and 23 to remove the predicted signal peptide (Bendtsen et al. 2004). There was a faint band above the 45-kDa band in the Endo H-digested samples (Figure 3, panel B, lane 1), suggesting that Hyal3 may have some complex *N*-linked glycans that are resistant to cleavage.

Analysis of the 412-amino-acid sequence of mouse Hyal3 predicted from the cDNA sequence (NP_821139.1) indicated that there are three potential *N*-linked glycosylation sites (<http://www.cbs.dtu.dk/services/NetNGlyc/>). Differences in glycan content could account for the various forms of Hyal3

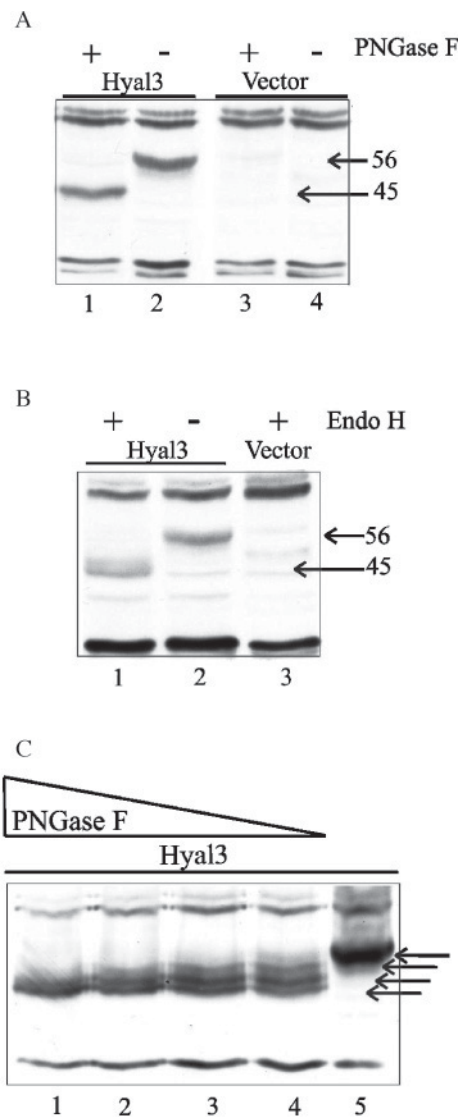


Fig. 3. Analysis of Hyal3 glycosylation. Lysates from BHK cells stably expressing pIRESHyal3 (Hyal3) or pIRESneo (vector) were digested with either PNGase F or Endo H, separated by SDS-PAGE, and analyzed by immunoblot with anti-Hyal3. The presence (+) or absence (-) of the glycosidases is indicated for each sample, and the molecular mass of the major protein bands detected is shown to the right. Panel A: complete digestion of Hyal3 with PNGase F shows conversion of a predominant 56-kDa form (lane 2) to a 45-kDa form (lane 1); these bands are absent in cells transfected with the empty vector (lanes 3 and 4). Panel B: complete digestion of Hyal3 with Endo H also shows conversion of the 56-kDa form (lane 2) to the 45-kDa form (lane 1), the latter of which is absent in Endo H-treated cells transfected with the empty vector (lane 3). Panel C: partial digestion of Hyal3 in lysates of BHK/Hyal3 cells with decreasing concentrations (units) of PNGase F (500 units, lane 1; 100 units, lane 2; 20 units, lane 3; 10 units, lane 4; and zero units, lane 5), showing appearance of four forms in partial digests (arrows).

that appeared in the transient expression lysates and variably in stably expressing cells. To assess this possibility, partial digestions were performed on BHK/Hyal3 lysates using various dilutions of PNGase F. As shown in Figure 3, panel C, four bands were produced by partial PNGase F digestion, indicating that there are likely three *N*-linked oligosaccharides, as predicted by the bioinformatic analyses.

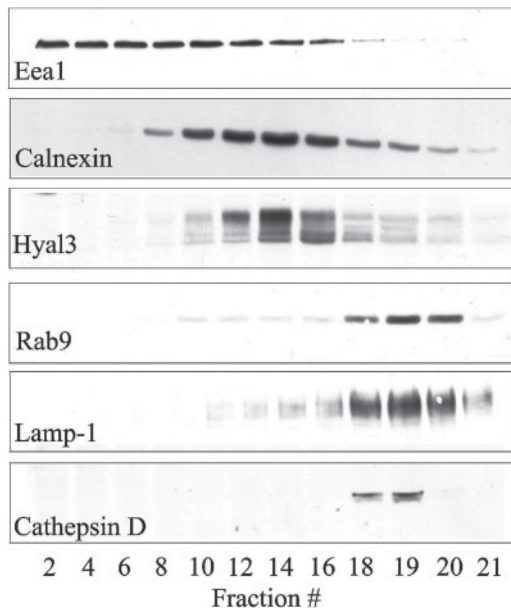


Fig. 4. Subcellular localization of Hyal3 by density gradient centrifugation. Lysates from BHK cells stably expressing Hyal3 were separated by Percoll density gradient centrifugation, and 21 fractions were collected from the gradient. Aliquots of the fractions were separated by SDS-PAGE and analyzed by immunoblot with either anti-Hyal3 or with antibodies against the cell compartment markers Lamp1, Eea-1, Calnexin, Rab9, and cathepsin D. Fractions are indicated at the bottom of the panels. Hyal3 is most abundant in fractions 12–16, overlapping with fractions containing the endoplasmic reticulum marker calnexin and the early endosome marker Eea1.

Localization of Hyal3 by density gradient centrifugation and immunofluorescence microscopy

To characterize the subcellular localization of Hyal3, we used Percoll gradient density centrifugation to separate the membrane-enclosed compartments of the cell. In a representative gradient analysis shown in Figure 4, Hyal3 was found in multiple fractions, spanning a range of gradient densities. The greatest amount of Hyal3 was found in the middle of the gradient overlapping with markers of the endoplasmic reticulum (calnexin) and early endosomes (early endosomal antigen 1 [Eea1]). However, small amounts of Hyal3 were detected in the same fractions as those containing the late endosomal/lysosomal markers ras-like GTPase 9 (Rab9) and lysosomal-associated membrane protein 1 (Lamp1), as well as the lysosomal marker, cathepsin D. Multiple electrophoretic forms of Hyal3 were sometimes detected in lysates (Figure 4). These forms showed differential distributions on the gradient, with the largest 56-kDa form most abundant in the lighter fractions (10–14) and the smaller forms contributing a larger proportion of the Hyal3 detected in the densities corresponding to the late endosomal/lysosomal fractions (18–20). Preliminary studies indicate that the number of detectable electrophoretic forms of Hyal3 varies under different conditions of cell growth (data not shown).

The subcellular localization of Hyal3 was examined further by conventional immunofluorescence microscopy. BHK cells stably expressing pIRESHyal3 (Hyal3) or pIRESNeo (vector) were incubated with antibodies toward Hyal3 in the presence or absence of the peptide used to generate the anti-Hyal3 anti-

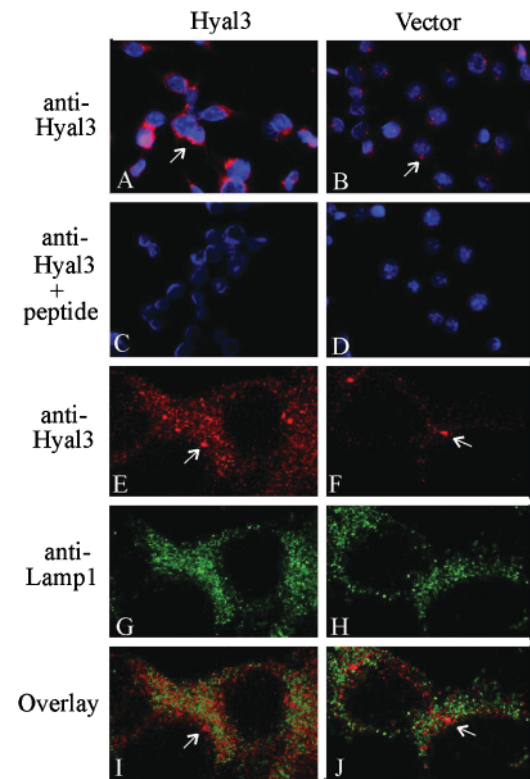


Fig. 5. Immunolocalization of Hyal3 by conventional and confocal immunofluorescence microscopy. BHK cells stably overexpressing pIRESHyal3 (Hyal3) or the pIRESneo vector (vector) were incubated with primary antibodies, anti-Hyal3 (dilution 1:250) or anti-Lamp1 (dilution 1:1000), and detected with fluorescently conjugated secondary antibodies to produce red fluorescence (Hyal3) and green fluorescence (Lamp1); the nuclei were counterstained with the blue-fluorescing dye, Hoeschst 33342 (0.1 μ g/mL). Some incubations were performed in the presence of the immunizing peptide (+ peptide in panels C and D) used to produce the Hyal3 antibody or without the primary antibody (data not shown). Panels A through D were visualized using conventional immunofluorescence microscopy. Panels E through J were visualized using confocal immunofluorescence microscopy. The arrows point to the intensely red fluorescent perinuclear granules that were detected by anti-Hyal3.

bodies used in this study. Anti-Hyal3 binding was then detected with Alexafluor555-conjugated secondary antibodies (red). As shown in panels A and B of Figure 5, Hyal3 was detected as red punctate fluorescence throughout the cytoplasm of both BHK cells overexpressing Hyal3 (Figure 5, panel A) and pIRESneo vector-transfected controls (Figure 5, panel B). Both endogenous Hyal3 in vector-transfected controls and overexpressed Hyal3 were detected as intensely fluorescing red perinuclear granules, although these structures were more numerous in the Hyal3-overexpressing cells (Figure 5, panel A) than in the control cells where generally only one granule was observed per cell (Figure 5, panel B). Both the endogenous and the overexpressed Hyal3 signals were effectively competed with the 14-residue peptide toward which the antibody was generated (Figure 5, panels C and D).

Further examination of the localization of Hyal3 was undertaken using confocal immunofluorescence microscopy (Figure 5, panels E–J). Consistent with the results above from the conventional immunofluorescence microscopy, Hyal3 (red) was

detected as punctate granules throughout the cytoplasm and as intense perinuclear granules in both BHK cells overexpressing Hyal3 (Figure 5, panel E) and controls stably transfected with the pIRESNeo vector (Figure 5, panel F). All granules were more numerous in the Hyal3-overexpressing cells although the distribution of both the endogenous and overexpressed Hyal3 protein appeared similar. When anti-Lamp1 was included in the incubation and detected with AlexaFluor488-conjugated secondary antibodies (green), Lamp1 was observed as punctate vesicles throughout the cytoplasm in both the Hyal3-overexpressing cells (Figure 5, panel G) and cells stably transfected with the pIRES-Neo vector (Figure 5, panel H). However, when the confocal images for Hyal3 and Lamp1 were overlaid, there was no colocalization of the two proteins detected (Figure 5, panels I and J).

Analysis of mouse Hyal3 activity

To assess the hyaluronidase activity of mouse Hyal3, lysates from transiently or stably transfected BHK cells were analyzed by zymography on native (Figure 6, panel A) and SDS-containing (Figure 6, panel B) polyacrylamide gels. As indicated by a clearing in the gel, the pIRESHyal3-expressing cells had a higher level of hyaluronidase activity than the cells transfected with the pIRESneo vector alone at pH 2.8 (Figure 6, panel A) and 3.8 (Figure 6, panel B). This activity was readily detectable between pH 2.8 and 4.1, and no activity was detectable at pH 5.0 or above (data not shown). However, as shown in Figure 6, panels A and B, the level of activity in the transient transfection lysates (lane 1) was lower than that in lysates from the stably expressing cells (lane 2), despite the detection of significantly higher levels of Hyal3 protein in transient expression lysates compared to stable expression lysates (Figure 2). This difference in expression versus activity was confirmed on repeated comparisons of the hyaluronidase activity associated with transiently transfected and stably expressed Hyal3 (data not shown). BHK cells stably expressing human HYAL1 (construction to be described elsewhere) were included as a positive control in these assays and exhibited saturating levels of activity under these conditions (Figure 6, panels A and B, lane 4).

To further examine the basis for the increased hyaluronidase activity observed in the BHK/Hyal3 lysates, pIRESHyal3 or the empty vector pIRESneo, was transiently expressed in mouse embryonic fibroblasts (MEFs) deficient in Hyal1 (Hyal1^{-/-}), and the level of hyaluronidase activity was determined using both zymography and aqueous assays. Hyaluronidase activity was not detected in the Hyal3- or vector-transfected cells by either zymography (data not shown) or aqueous assays (Figure 6, panel C, lanes 1 and 2), although the HA in the aqueous assay was completely degraded by a lysate from BHK cells stably expressing HYAL1, as indicated by the loss of the HA band in lane 3 of Figure 6, panel C. These analyses were repeated using different conditions for cell lysis (sonication, 1% Triton X-100, 1% 3-[(3-cholamidopropyl) dimethylammonio] propanesulfonic acid) and enzymatic assays (+/- 1 mM Ca²⁺, 50 mM, and 150 mM NaCl, formate- and acetate-based assay buffers, pH 3.5, 4.1, 5.5, and 7.4). However, no hyaluronidase activity could be detected under any of these conditions (data not shown).

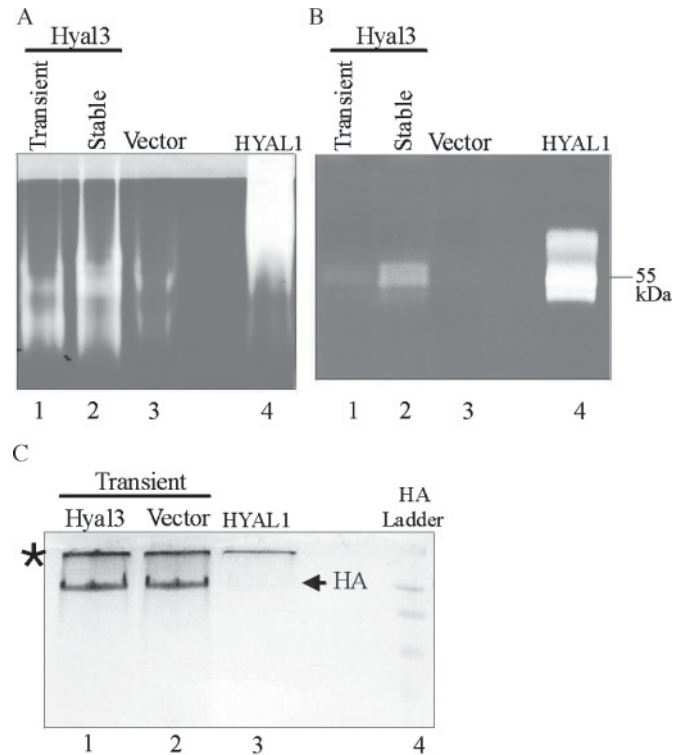


Fig. 6. Zymography or aqueous assay of hyaluronidase activity in lysates (60 µg of protein) from BHK cells or Hyal1^{-/-} MEFs stably or transiently expressing Hyal3 (pIRESHyal3) or vector (pIRESneo). Extracts from BHK cells stably expressing HYAL1 were used as a positive control for HA degradation. Greater areas of clearing (white areas) in lanes indicate higher levels of HA breakdown. Panels **A** and **B**: native PAGE followed by zymography of BHK expressing Hyal3, using the assay buffer at pH 2.8 (**A**) and SDS-PAGE followed by zymography of BHK expressing Hyal3 using the assay buffer at pH 3.8 (**B**), showing high HA breakdown by HYAL1 (**A**, **B**, lane 4), little HA breakdown in vector-transfected cells (**A**, **B**, lane 3), and higher levels of HA breakdown in lysates from stable (**A**, **B**, lane 2) compared with transient (**A**, **B**, lane 1) transfected cells. Panel **C**: aqueous assay of hyaluronidase activity in Hyal3-transfected Hyal1^{-/-} MEFs, showing complete breakdown of HA by HYAL1 (lane 3), and the absence of HA breakdown (arrow) by lysates from both vector-transfected (lane 2) and Hyal3-transfected (lane 1) cells. The asterisk indicates the band that results from the staining of DNA in the cell lysates. It should be noted that the presence of SDS in the sample buffer of extracts run on the SDS-PAGE gel results in the proteins migrating as discrete bands based on their molecular mass (panel **B**) while in the absence of SDS, the migration of the protein is influenced by other factors such as charge and results in a smeared band higher up in the gel (panel **A**).

Immunoblotting of Hyal1 and Hyal3 in transfected cells

The absence of detectable hyaluronidase activity in Hyal1^{-/-} MEFs transfected with pIRESHyal3 was unexpected. We performed immunoblot analysis using anti-Hyal3 on the Hyal1^{-/-} MEF cells that were transiently transfected with pIRESHyal3 and confirmed that Hyal3 was expressed in these cells (Figure 7, panel A, lane 1) and was not detected in the empty vector-transfected Hyal1^{-/-} MEF cells (Figure 7, panel A, lane 2). In conjunction with the data above demonstrating a lack of correlation between the level of Hyal3 protein and the level of hyaluronidase activity in pIRESHyal3 transfected BHK cells, we assessed another possible explanation for the increase in hyaluronidase activity. Given that Hyal1 is the primary somatic hyaluronidase, we decided to examine the expression

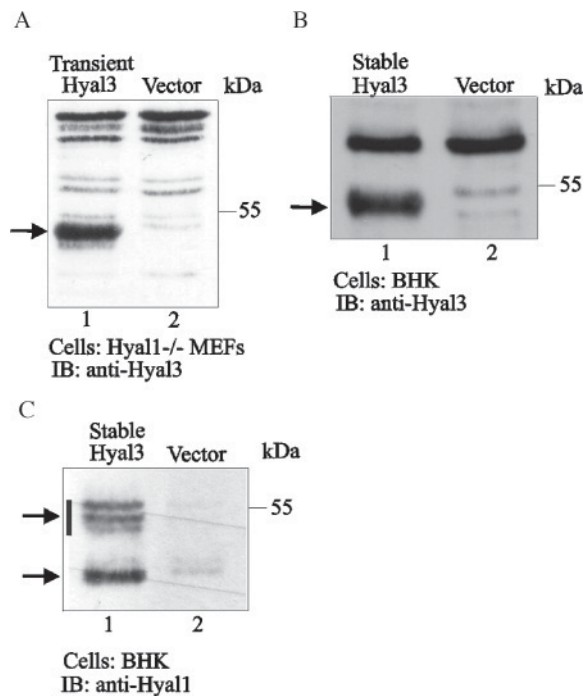


Fig. 7. Analysis of Hyal1 and Hyal3 protein in Hyal3 expressing cells. Lysates (50 μ g protein) from Hyal1^{-/-} MEFs transiently transfected with Hyal3 (pIRESHyal3) or vector (pIRESneo), and lysates from BHK cells stably transfected with the same vectors were separated by SDS-PAGE and immunoblots (IB) were performed with anti-Hyal3 or anti-Hyal1 as indicated. Panel A: detection of Hyal3 in Hyal3-transfected (arrow, lane 1) but not in control vector-transfected (lane 2) Hyal1^{-/-} MEFs. Panel B: detection of Hyal3 in BHK cells stably expressing Hyal3 (arrow, lane 1), and its absence in vector-transfected control BHK cells (lane 2). Panel C: blot showing increased levels of Hyal1 migrating as multiple forms in BHK cells stably expressing Hyal3 (arrows, lane 1) compared with weakly detectable levels in vector-transfected BHK cells (lane 2). Molecular weight markers are indicated to the right of each panel.

of the hamster Hyal1 protein in BHK cells stably expressing pIRESHyal3 and vector-transfected controls. Immunoblot analysis with anti-Hyal3 (Figure 7, panel B) and anti-Hyal1 (Figure 7, panel C) revealed much higher levels of both proteins (Figure 7, panels B and C, lane 1) than that observed in pIRESneo vector-transfected cells (Figure 7, panels B and C, lane 2). The increase in the hamster Hyal1 protein was consistent with the increased levels of acid-active hyaluronidase activity seen in BHK cells expressing pIRESHyal3 (Figure 6, lanes 1 and 2). The differing migration of Hyal1 in the BHK cells (Figure 6, lanes 1–3) compared to that of human HYAL1 (lane 4) is not surprising as differences in glycosylation will alter the migration of proteins on native gels and this has previously been observed for mouse Hyal1 in our own laboratory (data not shown).

To determine if the increase in Hyal1 activity was accompanied by an increase in the level of hamster Hyal1 mRNA, we used real-time PCR. A portion of the hamster Hyal1 sequence was determined to allow the design of a Taqman assay (described in the Materials and methods section) to quantitate hamster Hyal1 mRNA using real-time PCR (data not shown). Real-time analysis of the hamster Hyal1 transcript levels revealed an approximate 1.6-fold increase in the BHK cells stably

overexpressing Hyal3 compared with BHK cells stably transfected with the pIRESNeo vector. Taken together, these results suggest that the elevation in hyaluronidase activity observed in BHK cells overexpressing Hyal3 was at least in part due to the induction of Hyal1, but also possibly due to the stabilization of the Hyal1 protein.

Discussion

We have characterized the murine Hyal3 protein and examined its ability to degrade HA. To facilitate these studies, we developed overexpression systems to produce levels of Hyal3 protein adequate for analyses. This was necessary because endogenous levels of Hyal3 protein were not detectable in mouse tissues or cultured cells by western blot analysis with our antibody (data not shown), which is consistent with the broadly expressed but generally low levels of Hyal3 mRNA in mouse tissues (Shuttleworth et al. 2002). In our expression systems, we found that murine Hyal3 was a 45- to 56-kDa glycoprotein that is localized in a vesicular compartment. Surprisingly, Hyal3 did not appear to have any detectable hyaluronidase activity under our experimental conditions. However, Hyal3 overexpression did lead to an elevation in Hyal1 mRNA, protein, and activity levels, suggesting that Hyal3 may play some as yet unknown role in HA metabolism.

Analysis of Hyal3 produced in our overexpression system revealed between one and four protein forms ranging in size from 45 to 56 kDa. We have not yet specifically identified the conditions that led to the generation of one versus four forms, and it is therefore uncertain at present whether all of these forms exist endogenously. Nevertheless, complete PNGase F digestion of lysates that had one or two bands detectable by immunoblot resulted in only one 45-kDa band. Further, four Hyal3 bands could clearly be identified in partial digests generated with PNGase F. This indicated that the various forms of Hyal3 resulted from differences in *N*-glycan content. Since the smallest form of Hyal3 was more abundant in the region of Percoll gradients consistent with an endosomal or a lysosomal localization, it is possible that the oligosaccharides are removed by glycosidases during transit in one of these compartments, or during degradation.

The removal of nearly all of the oligosaccharides from Hyal3 with Endo H, which is specific for high mannose or hybrid *N*-linked oligosaccharides, indicated that the majority of the oligosaccharides on Hyal3 have a high mannose or hybrid structure. This observation suggests either that the Hyal3 protein enters a targeting pathway before the oligosaccharides are matured to complex structures, or that the structures are modified in a way that prevents further processing, such as the addition of a mannose-6-phosphate-targeting signal. Although it is possible that Hyal3 oligosaccharides might be processed through a mannose-6-phosphate-dependent route to the lysosome, we did not detect any colocalization of Hyal3 with the late endosomal/lysosomal marker Lamp1 using immunofluorescence. Further, in a previous study, HYAL1 was not targeted by a mannose-6-phosphate-dependent pathway (Natowicz and Wang 1996). An alternative explanation for the high mannose and hybrid sugars on Hyal3 is that it enters an unidentified vesicular structure that bypasses the mid- and trans-golgi apparatus, preventing further processing. Indeed, Hyal3 was found to be most concentrated in distinct perinuclear structures that did not

colocalize with Lamp1. Further investigations will be required to determine the identity of this perinuclear structure.

The degradation of HA is believed to take place in the lysosome (Roden et al. 1989). However, the localization of some hyaluronidases has been surprising, with PH-20 and HYAL2 both having plasma membrane and lysosomal forms (Cherr et al. 2001; Lepperdinger et al. 2001). By density gradient centrifugation, we found that the highest levels of Hyal3 localized to a region of the gradient between the early and late endosomes, similar in distribution to the endoplasmic reticulum marker calnexin. Detection of a large proportion of Hyal3 in this region of the gradient did not exclude it as a lysosomal enzyme, as such enzymes may have multiple stable subcellular localizations (Tomincio and Paigen 1975; Lusic and Paigen 1977). However, the failure to colocalize Hyal3 with Lamp1 suggests that if any Hyal3 does enter the lysosome, we cannot not detect it under the experimental conditions we employed for immunofluorescence microscopy. The Hyal3 detected in the central part of the gradient may be in transit to the late endosomes and/or another unique vesicular compartment. Unfortunately, Percoll gradients do not usually allow the late endosomes and lysosomes of BHK cells to be readily differentiated (Press et al. 1998). Mouse Hyal3 was not detected in the least dense fractions, where the plasma membranes are located (Press et al. 1998). Our results support the suggestion that Hyal3 is localized to a unique compartment, perhaps a structure dedicated to HA metabolism, the hyaluronasome, that has been speculated to exist (Stern 2003).

In a recently proposed model, the breakdown of HA is initiated extracellularly by HYAL2 and then continued intracellularly by HYAL1 (Stern 2003). Since we were unable to detect any hyaluronidase activity associated with Hyal3 using various conditions, it seems unlikely that Hyal3 initiates HA breakdown in a manner analogous to HYAL2 or continues HA breakdown in a fashion similar to HYAL1. However, HYAL2 activity has been difficult to detect (Lepperdinger et al. 1998), and it is possible that Hyal3 has very low hyaluronidase activity that escaped detection in our assay system. We also cannot rule out the possibility that there are other forms of mouse Hyal3 that are active as we only examined one clone representing a full-length form of Hyal3. In a previous *in vitro* study of human HYAL3, only the full-length form, and not its alternatively spliced forms, was found to be active (Lokeshwar et al. 2002). Consistent with our findings, however, human HYAL3 also had no detectable hyaluronidase activity when expressed in mammalian HEK293 cells (Harada and Takahashi 2007). It thus appears that HYAL3 would be unable to compensate for the HYAL1 deficiency seen in MPS IX patients (Triggs-Raine et al. 1999). Analysis of mouse models deficient in Hyal1 and/or Hyal3 will be necessary to assess these findings.

Curiously, BHK cells overexpressing Hyal3 in our studies displayed an increased level of hyaluronidase activity, Hyal1 protein, and Hyal1 mRNA. The complete basis of this increase is not yet clear; Hyal3 overexpression resulted in a 1.6-fold increase in Hyal1 mRNA. This may be consistent with Hyal3 serving as an intracellular HA-binding protein or transient plasma membrane receptor, as its overexpression may increase HA uptake and transport to the lysosome for degradation. This may lead to an increased demand for Hyal1 to degrade HA and in

turn, cause upregulation of Hyal1. The higher level of Hyal1 protein and activity observed in cells stably expressing Hyal3 compared to cells transiently expressing Hyal3 is consistent with an upregulation of Hyal1 in stably transfected cells during cell growth and proliferation, which is more restricted during the 40-h timeframe after transient transfection. To date, however, no GPI-anchored form of Hyal3 that might act as a receptor similar to HYAL2 has been recognized. Further, the classical link domain that mediates HA binding for many proteins (Day and Prestwich 2002) has not been identified in Hyal3. However, we have shown that Hyal3 stably expressed in BHK cells is able to bind HA *in vitro* (Triggs-Raine et al., in preparation).

In addition to increasing Hyal1 transcript levels, it is possible that Hyal3 overexpression increased Hyal1 protein and activity levels directly. Hyal3 may function to stabilize Hyal1 during transport through intracellular compartments. Many multimeric enzymes, including but not limited to β -hexosaminidase A and UDP-*N*-acetylglucosamine:lysosomal enzyme *N*-acetylglucosamine-1-phosphotransferase, require the presence of more than one subunit to be properly processed and targeted (Proia et al. 1984; Kudo and Canfield 2006). A well-known example is lysosomal neuraminidase that is active as a complex with protective protein/cathepsin A and β -galactosidase (Bonten and d'Azzo 2000). The three subunits are required for both intracellular transport and activation of neuraminidase (van der Spoel A. et al. 1998; Bonten and d'Azzo 2000). It is possible that Hyal3 acts as a chaperone or partner for Hyal1 and that increased Hyal3 expression leads to an increase in Hyal1 that is correctly folded and/or targeted through the cell to its destination. However, the lack of a direct correlation between Hyal3 levels and acid-active hyaluronidase activity when comparing stably and transient expressing cells suggests greater complexity than simply a one-to-one Hyal1–Hyal3 protein–protein interaction. As a result, Hyal1 levels may reach a maximal level that cannot be exceeded even with higher Hyal3 expression.

The pathway(s) and regulation of HA degradation appear to be more complex than would have been expected based on the comparison to the degradation pathways of other macromolecules. However, the broad distribution of HA and the critical functions that it has in a variety of processes may necessitate multiple hyaluronidases and mechanisms or regulation to provide the capacity to fine-tune the breakdown of HA.

Materials and methods

Antibodies

An epitope-purified rabbit polyclonal antibody (Cat. No. 38-3700) against mouse Hyal3 and the 14-amino-acid immunizing peptide were obtained from Invitrogen/Zymed. Mouse monoclonal antibodies were obtained against the MBP (New England Biolabs Ltd. [NEB], Pickering, ON), the endoplasmic reticulum marker calnexin (BD Biosciences, Mississauga, ON), the early endosomal marker Eea1 (BD Biosciences), the late endosomal markers Rab9 (Affinity Bioreagents, Golden, CO) and Lamp1 (Dr. Jean Gruenberg, University of Geneva), the lysosomal marker cathepsin D (BD Biosciences), and HYAL1 (Shuttleworth et al. 2002). Anti-rabbit Alexafluor 555 and anti-mouse Alexafluor 488 (Invitrogen) secondary antibodies were used for immunofluorescence microscopy.

Construction of expression plasmids

The mouse Hyal3 cDNA clone, IMAGE ID 3592874 (GenBank BE376250) was obtained from Invitrogen Canada Inc. (Burlington, ON). The full-length sequence of the *Hyal3* insert was determined and submitted to GenBank (accession no. NM_178020) as part of a previous study (Shuttleworth et al. 2002). A vector expressing the full-length mouse Hyal3-encoding cDNA was prepared by ligating a 1287-bp EcoN1/PleI (ends filled with Klenow) fragment from clone ID 3592874 into the EcoRV site of pIRESneo (BD Biosciences) to generate pIRESHyal3. The junctions of the vector were confirmed by DNA sequencing. Plasmids expressing hyaluronidase fusion proteins were prepared in pQE-80L (Qiagen Inc., Mississauga, ON) or pMalc2 (NEB) vectors. An N-terminal His-tag fusion with mouse Hyal3 was created by cloning the 1287-bp EcoN1/PleI fragment (above) into the SmaI site of pQE-80L to generate pQE-80L/Hyal3. For human HYAL3, a 1407-bp AflIII/TfiI fragment (ends filled with Klenow) was prepared from the full-length IMAGE clone ID 547239 and cloned into pMalc2 digested by HindIII (filled in by Klenow) to create pMalc2/HYAL3. For human HYAL2, a 928-bp fragment prepared by digesting the HYAL2-encoding IMAGE clone ID 38838 with PstI was cloned into pMalc2 digested by PstI to generate pMalc2/HYAL2. The human HYAL1 fusion was generated by cloning the 868-bp NcoI (filled in by Klenow)/BglIII fragment of IMAGE clone ID 650884 into pMalc2 digested by EcoRI (filled in by Klenow)/BamHI to generate pMalc2/HYAL1.

Fusion protein analysis

E. coli harboring the expression vectors of interest were grown to an OD of 0.6 at 600 nm and induced for 4 h with 0.2 mM isopropyl- β -D-thiogalactopyranoside. Cell pellets were collected and lysed with a Laemmli sample buffer (Laemmli 1970) containing 100 mM dithiothreitol. The human HYAL1-MBP and HYAL2-MBP fusions were isolated using amylose resin and following the protocol of NEB.

Cell culture and transfections

BHK cells were maintained in a minimal essential medium (alpha modification) containing 10% fetal bovine serum and 100 U/mL penicillin–streptomycin. Mouse embryonic fibroblasts were prepared from Hyal1-deficient mice (B6.129 \times 1-*Hyal1*^{tm1Stn}/Mmcd, Mutant Mouse Regional Resource Centre) using standard procedures (Nagy et al. 2003) and grown in Delbecco's minimal essential medium supplemented as above. These cells were immortalized by transfection with a plasmid expressing the large T-antigen.

Transfections of BHK cells were performed at approximately 85% confluence with 7 μ g of pIRESHyal3 or pIRESneo plasmid per 60-mm culture dish using Lipofectamine 2000 (Invitrogen Canada) following the manufacturer's specifications. Cells were collected at 40 h post-transfection. To prepare BHK cells stably expressing mouse Hyal3, the cells were diluted at 24 h post-transfection in media supplemented with 800 μ g/mL geneticin (G418) for selection. After 14 days of growth in G418, 45 colonies were picked and analyzed for Hyal3 expression by immunoblot analysis. Two clones stably expressing Hyal3 (BHK/Hyal3) and several clones stably transfected with the empty vector (BHK/pIRESneo) were identified and stored for future studies.

For MEF cells, transfection was performed in suspension using a modified protocol of Bode (Bode et al. 2003). Briefly, 5 μ g plasmid/15 μ L Lipofectamine were used to prepare complexes in OptiMEM (Invitrogen) following the manufacturer's instructions. After dilution in OptiMEM to 300 μ L, the lipid complexes were added to an equal volume of Hyal1^{-/-} MEFs that were collected from a confluent 100-mm plate into 3 mL of OptiMEM. This mixture was diluted with 1.0 mL of antibiotic-free medium and plated in a 60-mm dish. The media was replaced at 18 h and incubation was continued for an additional 24 h. Cells were then collected in phosphate-buffered saline (PBS) for further assays.

Immunoblot analysis

Cell lysates were separated by sodium dodecyl sulfate–polyacrylamide gel electrophoresis (SDS–PAGE) and transferred to nitrocellulose using 10 mM 3-(cyclohexylamino)-propanesulfonic acid, 10% methanol, pH 11 for Eea1, Lamp1, Calnexin, Hyal3, and Hyal1, and the method of Towbin et al. (1979) for cathepsin D and Rab9. Membranes were blocked with 5% skim milk powder in 10 mM Tris, 150 mM NaCl, pH 7.5, tris-buffered saline (TBS) containing 0.1% Tween 20. Primary antibody (1 μ g/mL for Hyal3; 1:2000 for MBP; 1:250 for Calnexin; 1:2500 for Eea1; 1:250 for Rab9, 1:200 for Lamp1; 1:1000 for cathepsin D; and 1:1000 for HYAL1) incubations were carried out overnight at 4°C or for 2 h at room temperature followed by 1 h in the secondary antibody (1/15,000 dilution), in the same solution. Horseradish peroxidase-conjugated secondary antibodies were purchased from Jackson ImmunoResearch Laboratories Inc. (Westgrove, PA). Reactive bands were detected with enhanced chemiluminescence (Pierce Biotechnology, Rockford IL).

Glycosidase digestions of Hyal3

BHK/Hyal3 or BHK/pIRESneo cells were washed with PBS and harvested in PBS containing 1% Triton X-100 and a protease inhibitor cocktail for mammalian cell lysates (Sigma-Aldrich Canada, Oakville, ON). Aliquots (50 μ g protein) were digested overnight at 37°C with either PNGase F (NEB) at pH 7.4 or Endo H (NEB) at pH 5.5 as described (Sambrook and Russell 2001) in a total volume of 25 μ L. For complete digestions 500 U of PNGase F or 2000 U of Endo H were used. Lysates were separated by SDS–PAGE on 7.5% gels and analyzed by immunoblot (see above).

Subcellular fractionation of BHK/Hyal3 cells

Subcellular fractionation of BHK/Hyal3 cells on Percoll gradients was carried out as described by Rosenfeld et al. (2001) with some modifications. Plated cells were grown to ~80% confluence, washed three times with PBS, and then scraped into a SHE buffer (0.25 M sucrose, 20 mM 4-(2-hydroxyethyl)-1-piperazineethanesulfonic acid, and 2 mM ethylene diamine tetraacetic acid pH 7.4). The suspended cells were washed once more with the SHE buffer and then homogenized in three volumes of the SHE buffer containing protease inhibitors by repeated passages through a 26-G needle. The homogenate was centrifuged at 1000 \times g for 10 min to obtain a post-nuclear supernatant, which was overlaid onto a solution of 25% Percoll in 1 \times SHE and centrifuged at 36,000 \times g for 45 min in a Beckmann 70.1 Ti rotor at 4°C. Fractions (15 drops) were

collected from the top of the gradient by the upward displacement of the gradient with 60% sucrose pumped through the bottom of the tube. Samples were separated by SDS–PAGE, and Hyal3 or organelle markers were detected by immunoblotting.

Immunofluorescence

BHK/Hyal3 or BHK/pIRESNeo cells were grown to the desired confluency on glass cover slips in 35-mm culture dishes. The cover slips were washed three times with cold PBS, and then fixed for 10 min at -20°C in 100% methanol. After washing in PBS, the cover slips were blocked for 1 h with 3% bovine serum albumin in TBS containing 0.05% Tween 20 (TTBS), followed by 1 h with anti-Hyal3 that had been preabsorbed for 6 h with 100 μg of lysate prepared from BHK/pIRES per 1 μg anti-Hyal3. To confirm the specificity of the antibody labeling, controls included incubation of the cells with the anti-Hyal3 that has been preincubated with the immunizing peptide (10 μg per μg of an anti-Hyal3 antibody) and incubation omitting the primary antibody. For colabeling, anti-Lamp1 was included in some incubations. After incubation with the primary antibodies, the cover slips were washed with TTBS and incubated with the secondary antibodies anti-rabbit Alexafluor 555 (for Hyal3) and where applicable anti-mouse Alexafluor 488 (for Lamp1). The cover slips were washed as above and mounted on slides with ProLong Gold (Invitrogen). Slides were examined by either a Zeiss conventional fluorescence microscope or an Olympus confocal microscope.

Hyaluronidase activity assays

Zymography was performed as previously described (Miura et al. 1995) but with some modifications. Briefly, cell lysates (60 μg protein) were separated by PAGE (SDS/nonreducing or native) on 7% gels containing 0.18 mg/mL human umbilical cord HA (Sigma Aldrich Cat No. H1876) at 20 mA for approximately 1 h at 4°C . SDS/nonreducing gels were incubated in 3% Triton X-100 for 2 h (two changes of detergent) before proceeding to the incubation in an assay buffer. All gels were equilibrated in the assay buffer (100 mM sodium formate, 150 mM NaCl, 0.1% Triton X-100, pH 3.8, or other pH as required) for 30 min at room temperature and subsequently incubated overnight in the same buffer at 37°C . After incubation, gels were treated with 0.2 $\mu\text{g}/\text{mL}$ proteinase K in a 20 mM Tris buffer (pH 8.0) for 4 h, rinsed with distilled water, and stained sequentially with 0.5% alcian blue in 3% acetic acid and 0.1% Coomassie blue in 30% methanol–10% acetic acid.

Aqueous assays for hyaluronidase activity were performed in a 100 mM formate buffer (pH 3.7) containing 75 mM NaCl and 0.5 μg of SelectHA(tm)150K (Associates of Cape Cod, Inc., MA). Lysate (50 μg protein) was added and the incubation was carried out at 37°C for 18 h. The products were analyzed by PAGE on a 10% gel, followed by visualization with 0.005% Stains-All prepared in 15 mM Tris (pH 8.8) containing 5% formamide and 25% isopropanol.

Real-time PCR

Total RNA was isolated from BHK cells using acidic phenol extraction (Sambrook and Russel 2001). The quantity and purity of RNA was assessed using the $A_{260}/_{280}$ optical density ratio. RNA was treated with TURBO DNA-free (Ambion Inc., Austin, TX) and used for cDNA production by random primer extension us-

ing Superscript III (Invitrogen) according to the manufacturer's instructions. A custom Taqman Gene Expression assay (Applied Biosystems Inc., Foster City, CA) for hamster *Hyal1* (forward [CGTCTCTATCCCAGTGTTCACCT], reverse [GCTGAGCCTCCCTGTTGT], probe [CCTGCGGCACTCAT]) was performed in triplicate using 50 ng of cDNA. A mouse *Hprt1* Taqman Gene Expression assay (Mm00446968_m1; Applied Biosystems Inc.) was used to normalize for cDNA loading. Gene Expression assays were performed using an Applied Biosystems 7300 Real-Time PCR system under standard cycling conditions (initial denaturing steps: 50.0°C for 2 min; 95.0°C for 10 min; Cycling conditions [40 \times]: 95°C for 15 s; 60.0°C for 1 min). Relative transcript levels were determined using the comparative Ct method with BHK/pIRESNeo RNA as the calibrator (Livak and Schmittgen 2001).

Funding

The Canadian Institutes of Health Research (MOP-15463 to BTR); The Garrod Foundation (to BTR and SP); DM was supported by an MHRC studentship.

Acknowledgements

The authors thank Nehal Patel, Tim Salo, Gerald Stelmack, and Sunita Khatkar for technical assistance, Dr. Jean Gruenberg for the gift of Lamp1 antibody, and Dr. Marvin Natowicz for critical review of the manuscript.

Conflict of interest statement

Dr. James Nagy is a paid consultant for Invitrogen/Zyomed, which was the source of the anti-Hyal3 antibody.

Abbreviations

BHK, Baby Hamster Kidney; Eea1, early endosomal antigen 1; Endo H, endoglycosidase H; *E. coli*, *Escherichia coli*; G418, geneticin; GPI, glycosylphosphatidylinositol; HA, hyaluronan; HYAL1, human hyaluronidase 1; HYAL2, human hyaluronidase 2; HYAL3, human hyaluronidase 3; Hyal1, mouse hyaluronidase 1; Hyal2, mouse hyaluronidase 2; Hyal3, mouse hyaluronidase 3; IB, immunoblot; Lamp1, lysosome-associated membrane protein 1; MBP, maltose binding protein; MEF, mouse embryonic fibroblast; MPS IX, Mucopolysaccharidosis IX; NEB, New England Biolabs; PBS, phosphate-buffered saline; PNGase F, peptide N-glycosidase F; rab9, ras-like GTPase 9; SDS–PAGE, sodium dodecyl sulfate polyacrylamide gel electrophoresis; TBS, tris-buffered saline; TTBS, tris-buffered saline containing 0.05% Tween 20.

References

- Baba D, Kashiwabara S, Honda A, Yamagata K, Wu Q, Ikawa M, Okabe M, Baba T. 2002. Mouse sperm lacking cell surface hyaluronidase PH-20 can pass through the layer of cumulus cells and fertilize the egg. *J Biol Chem.* 277:30310–30314.
- Bendtsen JD, Nielsen H, von Heijne G, Brunak S. 2004. Improved prediction of signal peptides: SignalP 3.0. *J Mol Biol.* 340:783–795.

- Bode JG, Schweigart J, Kehrmann J, Ehrling C, Schaper F, Heinrich PC, Haussinger D. 2003. TNF- α induces tyrosine phosphorylation and recruitment of the Src homology protein-tyrosine phosphatase 2 to the gp130 signal-transducing subunit of the IL-6 receptor complex. *J Immunol.* 171:257–266.
- Bonten EJ, d'Azzo A. 2000. Lysosomal neuraminidase. Catalytic activation in insect cells is controlled by the protective protein/cathepsin A. *J Biol Chem.* 275:37657–37663.
- Bourguignon LY, Singleton PA, Diedrich F, Stern R, Gilad E. 2004. CD44 Interaction with Na⁺-H⁺ exchanger (NHE1) creates acidic microenvironments leading to hyaluronidase-2 and cathepsin B activation and breast tumor cell invasion. *J Biol Chem.* 279:26991–27007.
- Bowness JM, Tan YH. 1968. Chromatographic distinction between hyaluronidases from human serum and ovine testes. *Biochim Biophys Acta.* 151:288–290.
- Cherr GN, Yudin AI, Overstreet JW. 2001. The dual functions of GPI-anchored PH-20: Hyaluronidase and intracellular signaling. *Matrix Biol.* 20:515–525.
- Csoka AB, Frost GI, Stern R. 2001. The six hyaluronidase-like genes in the human and mouse genomes. *Matrix Biol.* 20:499–508.
- Csoka A, Scherer SE, Stern R. 1999. Expression analysis of six paralogous human hyaluronidase genes clustered on chromosomes 3p21 and 7q31. *Genomics.* 60:356–361.
- Day AJ, Prestwich GD. 2002. Hyaluronan-binding proteins: Tying up the giant. *J Biol Chem.* 277:4585–4588.
- Fraser JRE, Laurent TC, Laurent UBG. 1997. Hyaluronan: Its nature, distribution, functions and turnover. *J Int Med.* 242:27–33.
- Frost GI, Csoka TB, Wong T, Stern R. 1997. Purification, cloning, and expression of human plasma hyaluronidase. *Biochem Biophys Res Commun.* 236:10–15.
- Gmachl M, Sagan S, Ketter S, Kreil G. 1993. The human sperm protein PH-20 has hyaluronidase activity. *FEBS Lett.* 336:545–548.
- Harada H, Takahashi M. 2007. CD44-dependent intracellular and extracellular catabolism of hyaluronic acid by hyaluronidase-1 and -2. *J. Biol. Chem.* 282:5597–5607.
- Kim E, Baba D, Kimura M, Yamashita M, Kashiwabara S, Baba T. 2005. Identification of a hyaluronidase, Hyal5, involved in penetration of mouse sperm through cumulus mass. *Proc Natl Acad Sci USA.* 102:18028–18033.
- Kosaki R, Watanabe K, Yamaguchi Y. 1999. Overproduction of hyaluronan by expression of the hyaluronan synthase Has2 enhances anchorage-independent growth and tumorigenicity. *Cancer Res.* 59:1141–1145.
- Kudo M, Canfield WM. 2006. Structural requirements for efficient processing and activation of recombinant human UDP-*N*-acetylglucosamine: lysosomal-enzyme-*N*-acetylglucosamine-1-phosphotransferase. *J Biol Chem.* 281:11761–11768.
- Laemmli UK. 1970. Cleavage of structural proteins during the assembly of the head of bacteriophage T4. *Nature.* 227:680–685.
- Lee JY, Spicer AP. 2000. Hyaluronan: A multifunctional, megaDalton, stealth molecule. *Curr Opin Cell Biol.* 12:581–586.
- Lepperdinger G, Mullegger J, Kreil G. 2001. Hyal2—less active, but more versatile? *Matrix Biol.* 20:509–514.
- Lepperdinger G, Strobl B, Kreil G. 1998. *HYAL2*, a human gene expressed in many cells, encodes a lysosomal hyaluronidase with a novel type of specificity. *J Biol Chem.* 273:22466–22470.
- Livak KJ, Schmittgen TD. 2001. Analysis of relative gene expression data using real-time quantitative PCR and the 2(-Delta Delta C(T)) Method. *Methods.* 25:402–408.
- Lokeshwar VB, Schroeder GL, Carey RI, Soloway MS, Iida N. 2002. Regulation of hyaluronidase activity by alternative mRNA splicing. *J Biol Chem.* 277:33654–33663.
- Lusis AJ, Paigen K. 1977. Relationships between levels of membrane-bound glucuronidase and the associated protein egasyn in mouse tissues. *J Cell Biol.* 73:728–735.
- McCourt PA. 1999. How does the hyaluronan scrap-yard operate? *Matrix Biol.* 18:427–432.
- Meyer MF, Kreil G, Aschauer H. 1997. The soluble hyaluronidase from bull testes is a fragment of the membrane-bound PH-20 enzyme. *FEBS Lett.* 413:385–388.
- Miller KA, Shao M, Martin-DeLeon PA. 2007. Hyalpl1 in murine sperm function: Evidence for unique and overlapping functions with other reproductive hyaluronidases. *J Androl.* 28:67–76.
- Miura RO, Yamagata S, Miura Y, Harada T, Yamagata T. 1995. Analysis of glycosaminoglycan-degrading enzymes by substrate gel electrophoresis (zymography). *Anal Biochem.* 225:333–340.
- Nagy A, Gertsenstein M, Vintersten K, Behringer R. 2003. Manipulating the Mouse Embryo. Cold Spring Harbor (NY): Cold Spring Harbor Laboratory Press. p. 371
- Natowicz MR, Short MP, Wang Y, Dickerson GR, Gebhardt MC, Rosenthal DI, Sims KB, Rosenberg AE. 1996. Clinical and biochemical manifestations of hyaluronidase deficiency. *New Engl J Med.* 335:1029–1033.
- Natowicz MR, Wang Y. 1996. Plasma hyaluronidase activity in mucopolipidoses II and III: Marked differences from other lysosomal enzymes. *Am J Med Genet.* 65:209–212.
- Press B, Feng Y, Hoflack B, Wandinger-Ness A. 1998. Mutant Rab7 causes the accumulation of cathepsin D and cation-independent mannose-6-phosphate receptor in an early endocytic compartment. *J Cell Biol* 140:1075–1089.
- Proia RL, d'Azzo A, Neufeld EF. 1984. Association of a- and b-subunits during the biosynthesis of b-hexosaminidase in cultured human fibroblasts. *J Biol Chem* 259:3350–3354.
- Rai SK, Duh FM, Vigdorovich V, Danilkovitch-Miagkova A, Lerman MI, Miller AD. 2001. Candidate tumor suppressor *HYAL2* is a glycosylphosphatidylinositol (GPI)-anchored cell-surface receptor for jaagsiekte sheep retrovirus, the envelope protein of which mediates oncogenic transformation. *Proc Natl Acad Sci USA.* 98:4443–4448.
- Reitinger S, Laschober GT, Fehrer C, Greiderer B, Lepperdinger G. 2007. Mouse testicular hyaluronidase-like proteins, SPAM1 and Hyal5 but not HyalP1 degrade hyaluronan. *Biochem J.* 401:85.
- Roden L, Campbell P, Fraser JRE, Laurent TC, Pertoft H, Thompson JN. 1989. Enzymic pathways of hyaluronan catabolism. *Ciba Found Symp.* 143:60–86.
- Rosenfeld JL, Moore RH, Zimmer KP, Alpizar-Foster E, Dai W, Zarka MN, Knoll BJ. 2001. Lysosome proteins are redistributed during expression of a GTP-hydrolysis-defective rab5a. *J Cell Sci.* 114:4499–4508.
- Sambrook J, Russel DW. 2001. Molecular Cloning: A Laboratory Manual. Cold Spring Harbor (NY): Cold Spring Harbor Laboratory Press.
- Seaton GJ, Hall L, Jones R. 2000. Rat sperm 2B1 glycoprotein (PH20) contains a C-terminal sequence motif for attachment of a glycosyl phosphatidylinositol anchor. Effects of endoproteolytic cleavage on hyaluronidase activity. *Biol Reprod.* 62:1667–1676.
- Shuttleworth TL, Wilson MD, Wicklow BA, Wilkins JA, Triggs-Raine BL. 2002. Characterization of the murine hyaluronidase gene region reveals complex organization and cotranscription of Hyal1 with downstream genes, Fus2 and Hyal3. *J Biol Chem.* 277:23008–23018.
- Stern R. 2003. Devising a pathway for hyaluronan catabolism: Are we there yet? *Glycobiology* 13:105R–115R.
- Tominco S, Paigen K. 1975. Egasyn, a protein complexed with microsomal beta-glucuronidase. *J Biol Chem* 250:1146–1148.
- Toole BP. 2000. Hyaluronan is not just a goo! *J Clin Invest.* 106:335–336.
- Towbin H, Staehelin T, Gordon J. 1979. Electrophoretic transfer of proteins from polyacrylamide gels to nitrocellulose sheets: Procedure and some applications. *Proc Natl Acad Sci USA.* 76:4350–4354.
- Triggs-Raine B, Salo T, Zhang H, Wicklow BA, Natowicz M. 1999. Mutations in *HYAL1*, a member of a tandemly distributed multigene family encoding disparate hyaluronidase activities, cause a newly described lysosomal disorder, mucopolysaccharidosis IX. *Proc Natl Acad Sci USA.* 96:6296–6300.
- Van Der Spoel A, Bonten E, d'Azzo A. 1998. Transport of human lysosomal neuraminidase to mature lysosomes requires protective protein/cathepsin A. *EMBO J* 17:1588–1597.